EVOLUTION & DEVELOPMENT 12:4, 373–382 (2010)
DOI: 10.1111/j.1525-142X.2010.00424.x

Early cranial patterning in the direct-developing frog *Eleutherodactylus coqui* revealed through gene expression

Ryan Kerney,[a] Joshua B. Gross,[b,1] and James Hanken[c]

[a]Department of Biology, Dalhousie University, 1355 Oxford St., Halifax, NS, Canada B3H 4J1
[b]Department of Genetics, Harvard Medical School, 77 Avenue Louis Pasteur, Boston, MA 02115, USA
[c]Museum of Comparative Zoology, Harvard University, 26 Oxford St., Cambridge, MA 02138, USA
*Author for correspondence (email: ryankerney@gmail.com)
[1]Present address: Department of Biological Sciences, University of Cincinnati, 312 College Drive, Cincinnati, OH 45221, USA.

SUMMARY Genetic and developmental alterations associated with the evolution of amphibian direct development remain largely unexplored. Specifically, little is known of the underlying expression of skeletal regulatory genes, which may reveal early modifications to cranial ontogeny in direct-developing species. We describe expression patterns of three key skeletal regulators (*runx2*, *sox9*, and *bmp4*) along with the cartilage-dominant collagen 2α1 gene (*col2a1*) during cranial development in the direct-developing anuran, *Eleutherodactylus coqui*. Expression patterns of these regulators reveal transient skeletogenic anlagen that correspond to larval cartilages, but which never fully form in *E. coqui*. Suprarostral anlagen in the frontonasal processes are detected through *runx2*, *sox9*, and *bmp4* expression. Previous studies have described these cartilages as missing from *Eleutherodactylus* cranial ontogeny. These transcriptionally active suprarostral anlagen fuse to the more posterior cranial trabeculae before they are detectable with *col2a1* staining or with the staining techniques used in earlier studies. Additionally, expression of *sox9* fails to reveal an early anterior connection between the palatoquadrate and the neurocranium, which is detectable through *sox9* staining in *Xenopus laevis* embryos (a metamorphosing species). Absence of this connection validates an instance of developmental repatterning, where the larval quadratocranial commissure cartilage is lost in *E. coqui*. Expression of *runx2* reveals dermal-bone precursors several developmental stages before their detection with alizarin red. This early expression of *runx2* correlates with the accelerated embryonic onset of bone formation characteristic of *E. coqui* and other direct-developing anurans, but which differs from the postembryonic bone formation of most metamorphosing species. Together these results provide an earlier depiction of cranial patterning in *E. coqui* by using earlier markers of skeletogenic cell differentiation. These data both validate and modify previously reported instances of larval recapitulation and developmental repatterning associated with the evolution of anuran direct development.

INTRODUCTION

All extant species of the neotropical frog genus *Eleutherodactylus* (Eleutherodactylidae) undergo "direct development," in contrast to the ancestral metamorphic anuran life history. Direct-developing *Eleutherodactylus* deposit small clutches of terrestrial eggs, which hatch as miniature froglets instead of aquatic tadpoles (Sampson 1900; Orton 1951; Hanken 1992). The evolution of direct development in *Eleutherodactylus coqui* correlates with loss of several tadpole-specific cranial cartilages and acceleration of adult bone and cartilage formation into embryonic stages (Lynn 1942; Hanken et al. 1992). This unique cranial development in *E. coqui* is not associated with any obvious changes in the timing and pattern of cranial neural-crest migration, which is relatively conserved between *E. coqui* and metamorphosing anurans (Moury and Hanken 1995). *E. coqui* does exhibit early *distal-less* mRNA expression (Fang and Elinson 1996) and novel immunoreactivity with an HNK-1 antibody in migratory cranial neural crest (Olsson et al. 2002). However, no causative link has been established between these early patterns of gene and protein expression and the loss of tadpole-specific cartilages.

Two previous studies have described cranial ontogeny of *Eleutherodactylus* in detail. Lynn (1942) examined cranial development of *Eleutherodactylus nubicola* using wax-plate reconstructions of histological sections (Fig. 1, B–F). More recently, Hanken et al. (1992) used immunohistochemistry with an anticollagen II antibody in whole-mount preparations of embryonic *E. coqui*. Both species lack tadpole-specific upper and lower jaw cartilages (suprarostral and infrarostral cartilages, respectively) as well as larval connections of the jaw

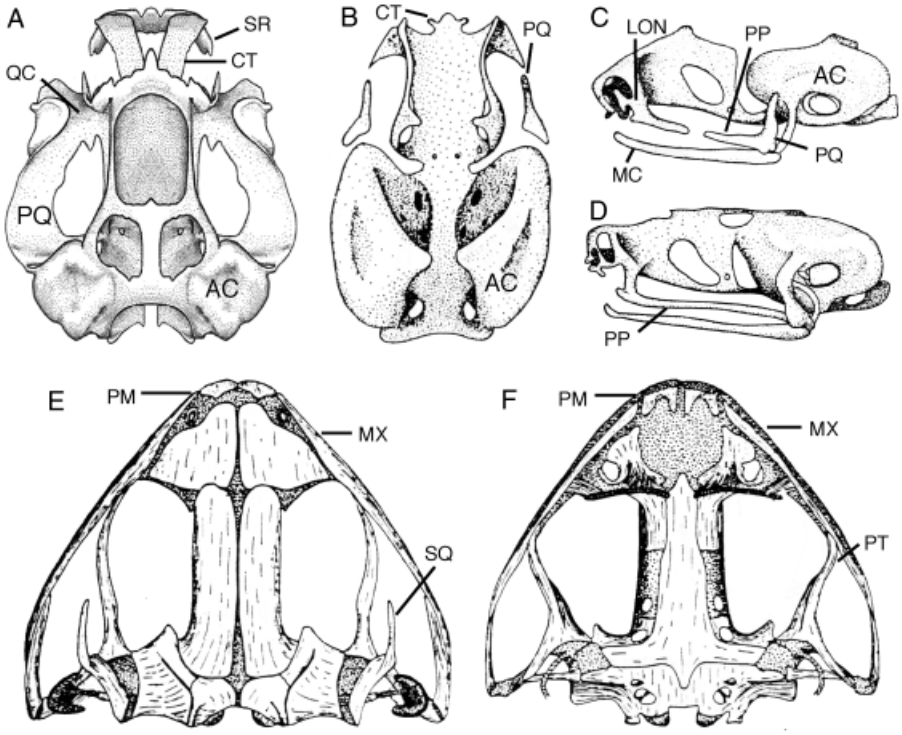

Fig. 1. Illustrations depicting cartilages and bones discussed in the text. (A) Larval cranium of *Rana temporaria*, dorsal view (modified from Pusey 1938). (B–F) Crania of *Eleutherodactylus nubicola* (modified from Lynn 1942). (B) Ten days prehatching, dorsal view; (C, D) 7 days pre- and 5 days posthatching, respectively, left-lateral views; (E, F) adult skull, dorsal and ventral views, respectively. Stippled regions in all panels are cartilage; unshaded regions in (E) and (F) are bone. AC, auditory capsule; CT, cranial trabeculae; LON, lamina orbitonasalis; MC, Meckel's cartilage; MX, maxilla; PM, premaxilla; PP, pterygoid process, which connects the palatoquadrate to the lamina orbitonasalis; PQ, palatoquadrate; PT, pterygoid; QC, quadratocranial commissure; SQ, squamosal; SR, suprarostral. Images are not depicted at the same scale.

suspension (palatoquadrate cartilage) to the neurocranium (through the quadratocranial commissure, otic, and ascending processes). Additionally, both species evince earlier formation, during embryogenesis, of typically postmetamorphic cartilages and bones. Tadpole-specific cartilages missing in *E. coqui* are presumably absent in all members of the direct-developing Terrarana clade, which includes Eleutherodactylidae (Heinicke et al. 2009). These cartilages (with the exception of the otic process) are found in other, metamorphosing nobleobatrachians (e.g., the nonfeeding tadpoles of *Flectonotus goeldii*: Hemiphractidae; Haas 1996), which form a Terrarana outgroup. Loss of these larval structures reflects evolutionary change in the initial (embryonic) patterning of the cranial skeleton and provides an example of "developmental repatterning" (sensu Hanken 1992), insofar as many corresponding adult features appear de novo and do not first recapitulate ancestral larval morphologies. The developmental basis of such evolutionary change is poorly understood, but presumably involves modifications to early cell and tissue interactions that lead to an altered cranial architecture in the embryo.

Comparative studies of skeletal patterning rely on early markers of cartilage and bone formation. The initiation of skeletogenesis is recognized traditionally by the first appearance of mesenchymal condensations in serial sections (Fell 1925; Holmgren 1933; Hanken and Hall 1988; Hall and Miyake 2000), which in chondrocytes is coincident with expression of the cartilage-dominant collagen *col2a1* (Hall 2005). Alternatively, early cartilage patterning can be revealed through the distribution of type-II collagen immunoreactivity (Linsenmayer and Hendrix 1980; Hanken et al. 1992; Seufert et al. 1994; Wake and Shubin 1998; Franssen et al. 2005), high-contrast microscopy (Shubin and Alberch 1986; Feduccia and Nowicki 2002; Franssen et al. 2005), or $^{35}SO_4$ uptake by chondroitin sulfate in cartilage (Searls 1965; Hinchliffe and Griffiths 1982). Endochondral bone replaces a pre-existing cartilaginous template, while intramembranous bones form directly from mesenchymal condensations. In both ossification processes osteoblast expression of *col1a1*, *osteocalcin*, *osteonectin*, *osteopontin*, and alkaline phosphatase activity (Sasano et al. 2000; Hall 2005) precede calcium deposition in the extracellular matrix, which is detectable through alizarin red and calcein (e.g., Kimmel et al. 2010). Each of these visualization techniques identifies different cellular behaviors during the developmental formation of the skeleton. The disadvantage of these techniques in assessing cartilage and bone patterning is that they rely on relatively late stages of skeletal cell differentiation. Therefore evolutionary patterning changes that are detected with these techniques may not reflect true differences in the *initial* patterning of skeletogenic cells. Here we describe earlier stages of cranial patterning of *E. coqui* than those reported in previous studies by examining mRNA expression of the chondrocyte and osteoblast regulator *runx2*, the neural crest and chondrocyte regulator *sox9*, and *col2a1*. The advantage of this approach is that it reveals differentiation of skeletal precursors several stages before the extracellular

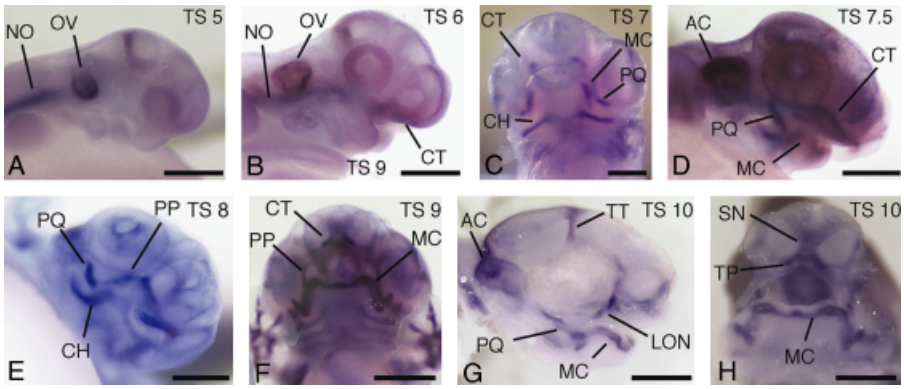

Fig. 2. *Col2a1* expression in the developing head reveals early cartilage patterning. (A, B, D, G) lateral; (C, F) ventral; (E) ventral oblique; and (H) anterior views. Eyes and skin have been removed from (G) and (H) to reveal underlying staining. Townsend-Stewart (TS) developmental stage is indicated in the top right corner of each frame. Additional abbreviations: CH, ceratohyal; NO, notochord; OV, otic vesicle; SN, septum nasi; TP, trabecular plate; TT, taenia tecti transversalis. Scale bars, 0.5 mm.

synthesis of cartilage and bone matrices. Expression of these skeletal differentiation regulators (*sox9* and *runx2*) corresponds to the initial morphological patterning of the skull, which is controlled by "upstream" pattern regulators, such as the signaling protein bmp4. Spatial and temporal expression of these genes confirms previously described instances of both cranial repatterning and recapitulation in *E. coqui*. Their expression also reveals novel recapitulation of tadpole morphologies, which were not detected in previous studies that relied on later markers of skeletal differentiation.

MATERIALS AND METHODS

Adult *E. coqui* were collected from the Caribbean National Forest near El Verde, Puerto Rico, under permission from the Departamento de Recursos Naturales y Ambientales (DRNA 03-IC-067). Rearing at Harvard University followed the Institutional Animal Care and Use Committee protocol 99-09. An Animal Welfare Assurance statement is on file with the university's Office for Laboratory Welfare (OLAW).

Cloning of *E. coqui runx2* (GenBank EF428557), *sox9* (EF428559), and *col2a1* (EF428558) and preparation of probes follow Kerney and Hanken (2008). *E. coqui bmp4* was amplified with the following degenerate primers: forward, 5′-(GCTTCTAGAGCTAATACAGTGTGTTCTTTYCAYCAYGARG-3′), and reverse, (5′-CCACATCCTTCCACCACCATRTCYTGRTA-3′). These primers amplified an 872 base-pair (bp) fragment, which is a subset of the previously accessioned 1203 bp *E. coqui bmp4* (NCBI accession number, AY525159). *Xenopus laevis sox9* in situ hybridization follows Kerney et al. (2007) and Spokony et al. (2002). *E. coqui* whole-mount in situ hybridization follows Kerney and Hanken (2008). Anatomical terminology is based on previous reports of skull development in *X. laevis* (Trueb and Hanken 1992) and *E. coqui* (Hanken et al. 1992).

RESULTS

Col2a1

Embryonic expression of *col2a1* mRNA reveals early morphology of the cartilaginous skeleton in *E. coqui*. At stage 5, there is nonskeletal expression of *col2a1* in the notochord and otic vesicles (Fig. 2A). During stage 6, *col2a1* is expressed in presumptive cranial trabeculae, which extend anteriorly to the mid nasal capsule region (Fig. 2B). The transcript is detectable early in stage 7 in cranial trabeculae, palatoquadrate precursors, and precursors of the lateral arms of the ceratohyal within the hyobranchial skeleton, with faint expression in lateral portions of Meckel's cartilage (Fig. 2C). *Col2a1*

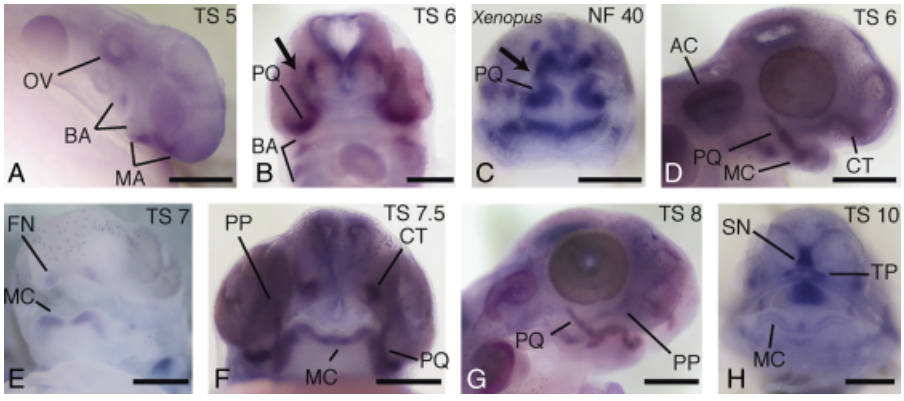

Fig. 3. *Sox9* expression in the developing head. (A, D, G) lateral; (B, E) ventral; and (F, H) anterior views. Eyes and skin have been removed from (H) to reveal underlying staining. (C) depicts a Nieuwkoop–Faber (1994) stage-40 (NF-40) *Xenopus laevis* embryo stained with the orthologous *sox9* probe, seen in ventral view. The cement gland has been removed to reveal underlying staining. Arrow in (B) indicates absence of quadratocranial commissure in early *Eleutherodactylus coqui*; arrow in (C) reveals this commissure in *Xenopus*. Additional abbreviations: BA, branchial-arch neural crest; FN, frontonasal process; MA, mandibular-arch neural crest. Scale bars, 0.5 mm.

expression in Meckel's cartilage extends toward the midline by stage 7.5 (Fig. 2D), when *col2a1* expression closely corresponds with *sox9* (Fig. 3F). Both genes are strongly expressed in the palatoquadrate, Meckel's cartilage, cranial trabeculae and auditory capsules. While the auditory capsules and Meckel's cartilage also have begun to form type-II collagen-rich condensations by this stage, only the cranial trabeculae have formed Alcian-positive cartilage (Hanken et al. 1992; Table 1).

Col2a1 continues to be strictly co-expressed with *sox9* in the developing skeleton during stages 8 and 9 (Figs. 2E and 3F). During stage 8, *col2a1* staining reveals an extended pterygoid process on each palatoquadrate cartilage; this process connects the palatoquadrate to the braincase through a lamina orbitonasalis (Fig. 2E). By stage 9, expression of *col2a1* in the anterior cranial trabeculae shifts toward the midline, with rostralmost ends directed ventrally (Fig. 2F). There also are dorsal extensions of *col2a1* expression in cranial trabeculae that later extend to form the septum nasi. Posterior to the septum, cranial trabeculae fuse in an anterior-to-posterior direction, forming the trabecular plate (not shown). The dorsal-most extension of the taenia tecti transversalis appears above the eye.

Col2a1 is strongly expressed throughout the entire cartilaginous head skeleton during stage 10. *Col2a1* is co-expressed with *sox9* in newly formed taenia tecti transversalis (Fig. 2G) and the septum nasi (Fig. 2H). Unlike *sox9*, *col2a1* expression along the ventral border of each lamina orbitonasalis persists through stage 10. The distribution of *col2a1* gives definition to each cartilage element, with no appreciable expression outside the cartilaginous skeleton. *Col2a1* mRNA expression now strictly colocalizes with type-II collagen antibody reactivity (Hanken et al. 1992; Table 1).

Sox9

Distribution of *sox9* mRNA reveals early cartilage anlagen and their neural-crest precursors. Early *sox9* expression labels migratory neural-crest streams along with the otic vesicles during stage 5 (Fig. 3A). However, unlike *col2a1*, *sox9* is not expressed in the notochord. Early in stage 6, *sox9* expression reveals well-defined palatoquadrate cartilage precursors in the mandibular arch and paired co-expression with *bmp4* and *runx2* in the frontonasal processes (Fig. 3B). *Sox9*-positive palatoquadrate anlagen extend dorsally but do not connect with the anterodorsal portions of *sox9* staining in the neurocranium (Fig. 3B). Palatoquadrate cartilages are connected to the anterior neurocranium through paired quadratocranial commissure cartilages in the metamorphic anuran, *X. laevis* (Trueb and Hanken 1992). *Sox9*-positive palatoquadrate and neurocranium anlagen are connected by paired *sox9*-positive quadratocranial commissures in *X. laevis* embryos (Fig. 3C). These commissures are tadpole-specific cartilages, which are found in many metamorphic anurans but missing in several direct-developing species, including *E. coqui* (reviewed in Kerney et al. 2007).

In later stage-6 embryos *sox9* expression expands to include the auditory capsules, Meckel's cartilage and cranial trabeculae anlagen (Fig. 3D). Palatoquadrate precursors extend anteriorly to connect with short Meckel's cartilage precursors in the "mid-metamorphic" pattern described by Hanken et al. (1992).

Sox9 expression continues to prefigure the cartilaginous skeleton throughout stage 7. Early in the stage, *sox9* is co-expressed with *runx2* in Meckel's cartilage and the frontonasal processes (Figs. 3E and 4C). Expression of *sox9* in more posterior cranial trabeculae extends anteriorly to connect with staining in the frontonasal processes by stage 7.5 (Fig. 3F). Pterygoid processes are also discernable through *sox9* expression by stage 7.5.

Sox9 expression changes little between stages 7.5 and 8. However, the pterygoid process of each palatoquadrate cartilage is fully revealed, connecting to the cranial trabeculae dorsally (Fig. 3G).

Table 1. The sequence and timing of formation of the notochord, otic vesicles, and cranial skeletal elements as assessed by different whole-mount staining techniques

	Alcian blue	Type-II collagen antibody	Col2a1	Sox9	Runx2
Stage 5		NO, OV	NO, OV	OV	
Stage 6			CT	AC, CT, FN, MC, PQ	CT, FN, MC, PQ
Stage 7	CT	AC, CT, MC	AC, MC, PQ	PP	PM[1]
Stage 8	AC, MC, PQ	PQ	LON, PP	LON	AN[1]
Stage 9	LON, PP, TP	LON, PP, TP, TT	TP, TT	TP, TT	SQ[1]
Stage 10	SN, TT	SN	SN	SN	MX[1]

Alcian blue and type-II collagen antibody staining methods are described by Hanken et al. (1992).

[1]Premaxillary, angulosplenial and squamosal bones are first detectable at stage 12, and maxillary bones at stage 13, through Hall-Brunt quadruple staining (Hall 1986) of serial sections (Hanken et al. 1992).

AC, auditory capsule; AN, angulosplenial; CT, cranial trabeculae; FN, frontonasal process; LON, lamina orbitonasalis; MC, Meckel's cartilage; MX, maxilla; NO, notochord; SN, septum nasi; OV, otic vesicle; PM, premaxilla; PP, pterygoid process; PQ, palatoquadrate; SQ, squamosal; TP, trabecular plate; TT, taenia tecti transversalis.

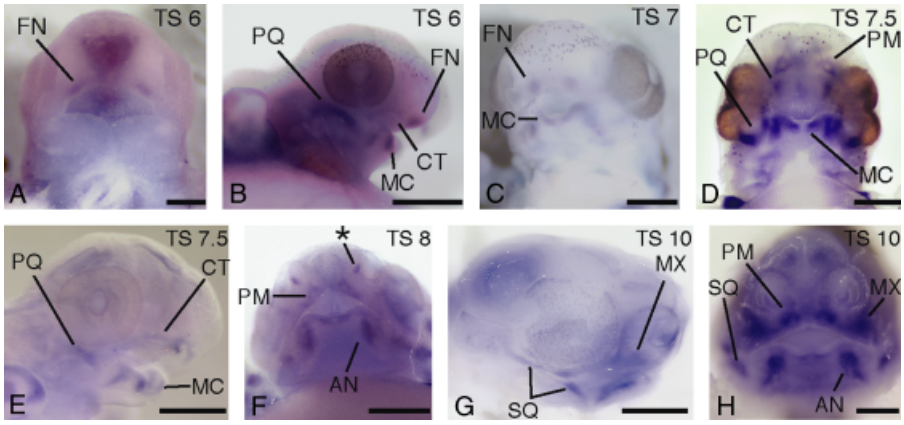

Fig. 4. *Runx2* expression in the developing head. (A, C, D, F) ventral; (B, E) lateral; and (H) anterior views. Eyes and skin have been removed from (G) and (H) to reveal underlying staining. Asterisk in (F) indicates transient *runx2* expression along the ventromedial border of the external nares during stage 8. Additional abbreviation: AN, angulosplenial precursor. Scale bars, 0.5 mm.

Sox9 and *col2a1* continue to be co-expressed in the presumptive skeleton during stage 9, with additional expression at this stage in the trabecular plate and taenia tecti transversalis (Table 1). The two genes continue to be expressed in cranial trabeculae and the septum nasi. However in contrast to *col2a1*, *sox9* expression weakens as new cartilages are formed. *Sox9* expression is faint in Meckel's cartilage by stage 10, despite strong *col2a1* expression (Fig. 3H).

Runx2

Runx2 is expressed initially in a subset of *sox9*-expressing cells. By stage 7, *runx2* and *sox9* are co-expressed in several skeletogenic anlagen. Their expression patterns diverge in subsequent stages. *Sox9* expression labels early chondrocytes, whereas *runx2* is expressed in differentiating osteoblasts.

Runx2 is not expressed in migratory neural crest, notochord, or otic vesicle during stage 5 (not shown). Its expression begins as paired clusters of cells in the frontonasal processes of early stage-6 embryos (Fig. 4A). Soon after these elements appear, *runx2* staining of palatoquadrate precursors becomes visible as broad, horizontal anlagen ventral to the eyes (Fig. 3B). *Runx2* also is co-expressed with *sox9* in precursors to Meckel's cartilage, and there is faint *runx2* staining in the cranial trabeculae.

Runx2 and *sox9* are co-expressed in the head during stage 7.0 (Figs. 3E and 4C). Both exhibit paired staining in the frontonasal processes, Meckel's cartilage and palatoquadrate precursors.

Meckel's cartilage and palatoquadrate precursors continue to co-express *runx2* and *sox9* by stage 7.5 (Fig. 4, D and E). However anterior *runx2* staining in frontonasal processes begins to form hollow triangular elements, which correspond to the position and form of the future premaxillary bones (Figs. 1, E–F, and 4D). These elements are not seen in *sox9* staining (Fig. 3F). Faint *runx2* staining also occurs in cranial trabeculae posterior to, and separate from, the presumptive premaxillae.

Runx2 expression becomes weaker in anteromedial portions of Meckel's cartilage by the beginning of stage 8

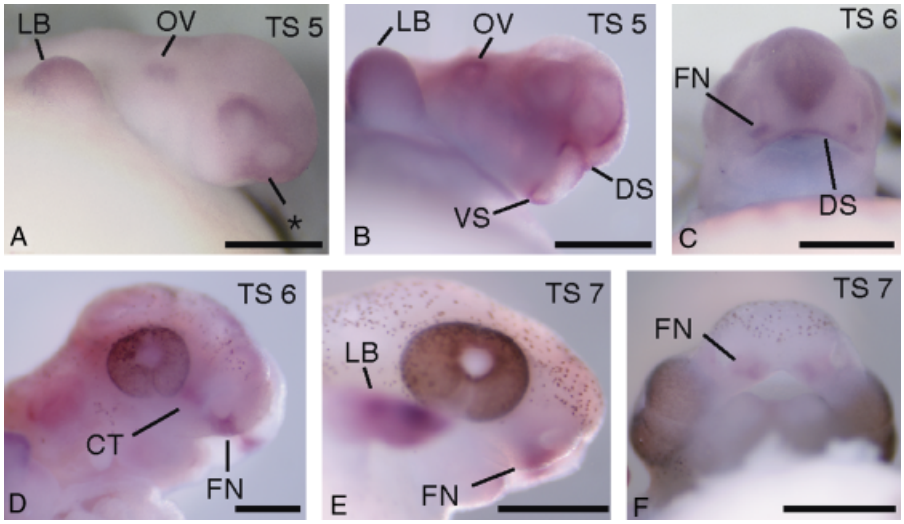

Fig. 5. *Bmp4* expression in the developing head. (A, B, D, E) lateral and (C, F) ventral views. Asterisk in (A) indicates early expression in the maxillary region of the stage-5 embryo. Additional abbreviations: DS, dorsal stomodeum; LB, limb bud; VS, ventral stomodeum. Scale bars, 0.5 mm.

(Fig. 4F). There is, however, strong *runx2* expression on the labial edges of posterolateral portions of Meckel's cartilage, which correspond to the presumptive angulosplenial bones. Expression in the anterior cranial trabeculae is also absent, and presumptive premaxillae remain triangular. Palatoquadrate precursors no longer express *runx2* staining anteriorly. Transient expression of *runx2* in the ventromedial borders of the external nares is only found during stage 8, and does not correspond to any specific cartilage or bone. By stage 10, expression of *runx2* in palatoquadrate cartilages is restricted to their posterior edges, which correspond to the future location of the paired squamosal bones.

Distribution of *runx2* by stage 10 prefigures several later-developing bones. There is strong expression in angulosplenial, premaxilla, and squamosal precursors (Fig. 4, G and H). Staining of paired squamosal condensations connect to the otic capsules posteriorly through their otic ramus and extend toward the lower jaw through their ventral ramus. Additional expression in the presumptive maxillae occurs anterior to the eyes, and diffuse staining is evident around the cartilaginous nasal capsules.

Bmp4

Bmp4 is broadly expressed in the maxillary region of the head and the otic vesicle by stage 5 (Fig. 5A). Expression becomes restricted to dorsal and ventral stomodeal ectoderm later in the stage (Fig. 5B). Dorsal stomodeal expression continues during stage 6, whereas expression disappears from the ventral stomodeum (Fig. 5C). During stage 6, paired *bmp4* expression appears in frontonasal processes, where *bmp4* is co-expressed with *runx2* and *sox9*. These regions are anterior to and separate from transient *bmp4* expression in cranial trabeculae (Fig. 5, C and D). More posterior cranial trabeculae expression disappears by stage 7, but frontonasal process expression persists (Fig. 5, E and F). *Bmp4* is not detected in the head during later developmental stages (data not shown).

DISCUSSION

A variety of whole-mount skeletal staining techniques are used to visualize cranial cartilage and bone development (Table 1). These techniques assay different aspects of cellular differentiation, revealing patterning at different stages of skeleton formation. For example, the presence of sulfated proteoglycans in the cartilaginous extracellular matrix is revealed using Alcian blue (Lev and Spicer 1964), whereas earlier deposition of collagen fibers can be detected with type-II collagen immunohistochemistry (Linsenmayer and Hendrix 1980). Successively earlier stages of cartilage differentiation can be visualized through in situ hybridizations that detect the type-II collagen precursor mRNA, *col2a1* (e.g., Su et al. 1991), or mRNA of the transcription factor *sox9* (e.g., Wright et al. 1995), the protein of which is required for *col2a1* transcription in chondrocytes (Bell et al. 1997). Additionally, *runx2* in situ hybridization stains early chondrocytes as well as presumptive ossification centers several developmental stages before they are detected by whole-mount staining with alizarin red (Table 1). Assaying earlier stages of skeletal cellular differentiation may reveal unexpected aspects of cranial patterning that are not observed with conventional staining techniques (e.g., Welten et al. 2005).

The missing suprarostral cartilages

Most metamorphosing tadpoles have paired suprarostral cartilages, which support the upper jaw. These cartilages are resorbed during metamorphosis, although some authors contend that they persist as the inferior prenasal cartilages of the adult (reviewed in Roček 2003). Distinctly paired suprarostral cartilages, however, are not present in either the family Pipidae, which includes *Xenopus* (Trueb and Hanken 1992), or the direct-developing *Eleutherodactylus* (Lynn 1942; Lynn and Lutz 1946; Hanken et al. 1992). Yet, early *runx2* and *sox9* expression in *Xenopus* reveal paired cellular anlagen that contribute to the unpaired suprarostral plate, which forms the upper larval jaw in the family Pipidae (Kerney et al. 2007). This implies that the plate is homologous to suprarostral cartilages of other metamorphosing species. These precursors fuse medially into a single plate and fuse posteriorly with the neurocranium, before formation of the histologically distinct cartilaginous anlagen (as described by Sadaghiani and Thiébaud 1987). In *Eleutherodactylus*, paired skeletal precursors in the frontonasal processes are not detectable through histology (Lynn 1942), Alcian blue or type-II collagen antibody staining (Hanken et al. 1992). Interestingly, other frog lineages that have convergently evolved direct-development do form transient suprarostral cartilages in the embryo, which are quickly resorbed before hatching (e.g., *Philautus*; Kerney et al. 2007), or form transient condensations attached to the anterior cranial trabeculae (e.g., *Breviceps*; Swanepoel 1970).

Early expression of *bmp4*, *sox9* and *runx2* in *E. coqui* reveal paired regions of staining in the frontonasal processes (Figs. 3E, 4, B–C, 5, C–F and 6), which are comparable to anterior regions of *runx2* and *sox9* staining in *X. laevis*. These regions correspond to the "missing" tadpole-specific suprarostral cartilages in *E. coqui*. As observed in *X. laevis*, this staining does not correspond to distinct paired anterior cartilages. Instead, the distribution of each gene changes as *col2a1*-positive cranial trabeculae extend anteriorly and cartilaginous extracellular matrix is produced (Fig. 6). *Bmp4* expression in the frontonasal mesenchyme disappears while *sox9* staining fuses posteriorly with *col2a1*-positive cranial

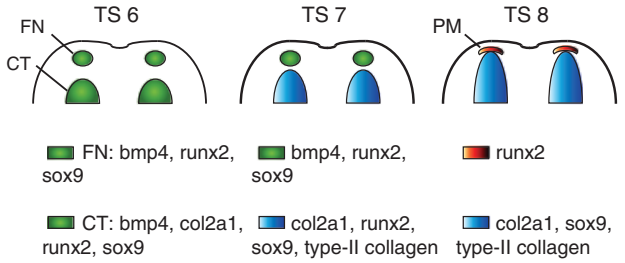

Fig. 6. Schematic depiction of the ethmoid region in coronal view, summarizing changes in gene expression between stages 6 and 8. Green indicates early skeletal anlagen that are detectable with gene expression (*bmp4*, *runx2*, and *sox9*), but have no type-II collagen positive extracellular matrix. Early cranial trabeculae (CT) also express *col2a1* mRNA, but not the type-II collagen protein. Blue indicates type-II collagen positive cartilage, based on previously reported whole-mount immunohistochemistry (Hanken et al. 1992). Red indicates runx2 expression in the future premaxillary bones (PM). Early anlagen express *bmp4* while later type-II collagen positive cartilage and dermal bone precursors do not. Anlagen of the advancing CT fuse with the frontonasal process anlagen (FN), while *runx2* expression becomes confined to the future premaxillae and *bmp4* expression dissipates.

trabeculae, and paired *runx2* staining assumes distinct hollow triangular shapes, which correspond to the future premaxillary bones. Coordinated changes in the expression patterns of these genes coincide with an anterior extension of type-II collagen-positive cranial trabeculae during stage 7 (Hanken et al. 1992).

Early expression of these genes in the frontonasal processes reveal separate paired precursors to the anterior neurocranium, which are among the first skeletogenic cells detectable in early embryos (Fig. 6). Similarly, in metamorphosing species such as *Rana temporaria*, the suprarostrals are among the first cranial cartilages to form during embryogenesis (Spemann 1898). Two distinct neural crest contributions have been mapped for the anterior ethmoid cartilage in zebrafish (*Danio rerio*). A separate anterior neural crest-derived population fuses to lateral and posterior cranial trabeculae in zebrafish before the cartilage begins to differentiate (Wada et al. 2005). It is possible that the paired anterior skeletal progenitors described in *X. laevis*, and now *E. coqui*, correspond to the anterior ethmoid precursors in zebrafish, given their shared developmental features. Both cartilage precursors appear in the anterior neurocranium and fuse to adjacent cartilage precursors before cartilage extracellular matrix formation. By extension, the suprarostral cartilages of most metamorphosing anuran tadpoles may also be derived from a distinct anterior crest population. Several early morphologists believed the suprarostrals originated as anterior extensions of the trabeculae (e.g., Stör 1882; reviewed in Roček 2003). If the anuran suprarostral cartilages are derived from a neural crest population that is homologous with the zebrafish ethmoid precursors, then a trabecular extension hypothesis would not be supported.

The missing quadratocranial commissure

A previously reported instance of developmental repatterning in *Eleutherodactylus* is the evolutionary loss of the larval quadratocranial commissure, a cartilaginous connection between the anterior palatoquadrate cartilage and cranial trabeculae in tadpoles of metamorphosing species (Fig. 1; Lynn 1942; Lynn and Lutz 1946; Hanken et al. 1992). In *Xenopus* embryos, *sox9*-expressing cells connect each anterior palatoquadrate precursor to cartilage precursors in the neurocranium, yet this connection never forms in *E. coqui* (Fig. 3). This failure of cartilage precursors to fuse precedes the absence of the quadratocranial commissure cartilage in embryonic *E. coqui*. Instead *sox9*-positive palatoquadrate anlagen later connect dorsally to the lamina orbitonasalis through the pterygoid process, which forms during metamorphosis in anurans with free-living tadpoles (Reiss 1998). This connection is visible during stage 8, in *sox9* in situ hybridizations, and during stage 9, through *col2a1* in situ hybridizations and type-II collagen antibody staining (Hanken et al. 1992).

Recapitulation versus repatterning

The term "repatterning" has seen several uses in studies of evolutionary developmental biology. Zelditch (2003) differentiates between temporal and spatial repatterning in the evolution of developmental processes. She points out that "repatterning" alone can be too inclusive, and therefore meaningless, in describing the developmental basis of morphological evolution. "Ontogenetic repatterning" is used to describe the new morphogenetic pathways that may evolve following the loss of developmental constraints. These include constraints on adult morphology associated with a metamorphic ontogeny in some taxa (Roth and Wake 1985; Wake and Roth 1989). Our use of "developmental repatterning" refers to reorganization of initial spatial patterning in the embryo, such that adult structures form *de novo* and not on templates provided by pre-existing larval components, which instead are absent or highly reduced (Hanken et al. 1992; Hanken et al. 1997). One instance of developmental repatterning reported here involves the complete absence of the quadratocranial commissure from the outset of *sox9*-detectable cartilage patterning. Instead, the adult connection between the jaw suspension and neurocranium, through the pterygoid process, forms at a later developmental stage without the preceding larval connection. This instance of repatterning suggests changes to upstream patterning mechanisms (e.g., the Dlx genes; Depew et al. 2002), instead of a simple acceleration of the ancestral metamorphic ontogeny during embryonic stages.

In *E. coqui*, evolutionary loss of the quadratocranial commissure represents a different mechanism from that which underlies the evolutionary loss of suprarostral cartilages. Our finding of previously undetectable skeletogenic precursors of the suprarostrals, in the early frontonasal processes, suggests that loss of these cartilages is attributable to a change in the timing of chondrocyte differentiation instead of patterning changes per se (repatterning). The suprarostrals are typically resorbed during metamorphosis in anuran species with a distinct free-living tadpole stage (Pusey 1938). In *E. coqui*, however, this change occurs in the early embryo, before cartilage extracellular matrix production (Hanken et al. 1992) or even expression of *col2a1* (Fig. 6). Earlier studies of *Eleutherodactylus* cranial patterning used histological or whole-mount staining techniques that could not detect these skeletogenic anlagen before they fused (Lynn 1942; Hanken et al. 1992). Instead of developmental repatterning, *E. coqui* undergoes embryonic recapitulation of both the larval suprarostral patterning mechanisms and subsequent metamorphic transformation of the suprarostral anlagen, before these anlagen are detectable with conventional techniques. The recapitulation of suprarostral precursors in *E. coqui* suggests that these elements play a conserved and possibly critical role in anuran cranial morphogenesis, even in species in which the corresponding cartilages are neither functional nor fully developed at any time of their life history.

Bmp4 expression

Bmp4 is a signaling molecule from the TGF-β superfamily. It is implicated in the morphogenesis (e.g., Foppiano et al. 2007) and evolution of maxillary (Abzhanov et al. 2004) and mandibular (Albertson et al. 2005) skeletal elements. Expression of *bmp4* in mouse (Semba et al. 2000) and chicken (Shigetani et al. 2000) is dynamic, rapidly changing between different tissue types during embryonic development. The pattern of *bmp4* expression in *E. coqui* also changes quickly within and between developmental stages (Fig. 5). Early pan-stomodeal expression in ectoderm and later expression in mesenchyme of frontonasal processes (Fig. 5C) is consistent with previous reports of an early ectodermal-to-mesenchymal change in *bmp4* expression in facial processes of Darwin's finches (Abzhanov et al. 2004). *Bmp4* co-expression with *runx2* and *sox9* in frontonasal processes also is consistent with its expression in prechondrogenic maxillary mesenchyme of large-billed finch species (e.g., *Geospiza magnirostris*) before cartilage extracellular matrix deposition. *Bmp4* expression in *E. coqui* maxillary mesenchyme disappears by stage 8, when anterior extensions of type-II collagen-positive cranial trabeculae reach their rostral-most limit (Fig. 6). The expression pattern of *bmp4* in this region suggests that this gene plays a role in craniofacial morphogenesis in *E. coqui*, as has been demonstrated in several other vertebrate groups (reviewed in Parsons and Albertson 2009). Further comparative research with metamorphosing outgroups is required to determine the extent to which changes in *bmp4* expression may account for evolutionary changes in cranial development in *E. coqui*.

Runx2 expression and embryonic bone formation

Embryonic distribution of *runx2* and *sox9* in *E. coqui* differs from that in the metamorphic frog, *X. laevis*. Whereas both genes are expressed during embryonic formation of the chondrocranium in *Xenopus*, expression of *sox9* and of *runx2* decrease dramatically as larval anlagen chondrify (Spokony et al. 2002; Kerney et al. 2007). *Sox9* and *col2a1* mRNA expression reappears during metamorphic formation of adult cartilage (Kerney et al. 2010), and *runx2* expression reappears during formation of adult bone (Moriishi et al. 2005). In *E. coqui*, *sox9* and *runx2* colocalize early in development in the presumptive chondrocranium, where they prefigure the distribution of *col2a1* (Table 1). However, *runx2* transitions from co-expression with *sox9* to a separate and distinct expression pattern, which corresponds to future elements of the bony skull. This transition begins during stage 7 and is complete by stage 10 (Fig. 4). A similar transition of *runx2* expression occurs in the limb skeleton of *E. coqui*. While both *runx2* and *sox9* are co-expressed initially in anlagen of long-bone elements, *runx2* expression is sequestered to developing long-bone perichondria and periostea also during stage 7 (Kerney and Hanken 2008).

E. coqui embryos undergo several developmental changes, often associated with metamorphosis, between stages 9 and 12 (Jennings and Hanken 1998; Callery and Elinson 2000a; Schlosser and Roth 1997). Further, *E. coqui* embryos treated with the thyroid inhibitor methimazole arrest development at stage 12 (Callery and Elinson 2000b). The transition of *runx2* expression to nascent osteoblasts occurs earlier (stage 7). Hence, *runx2* expression in osteoblast precursors may not be dependent on precocious activation of the thyroid axis in *E. coqui*.

Runx2 protein is essential for the formation of larval viscerocranial cartilages in *X. laevis* (Kerney et al. 2007) and zebrafish (Flores et al. 2006). While *runx2* staining does reveal early cranial cartilages in *E. coqui*, it does not stain the septum nasi. This adult cartilage is, however, apparent with *sox9* and *col2a1* staining (Figs. 2H and 3H). Absence of *runx2* staining indicates that this gene is not essential for differentiation of all adult cartilages. A clearer role for *runx2* in anuran cartilage differentiation awaits verification using assays of runx2 protein function (e.g., overexpression and knock-down experiments) during skeletal metamorphosis.

Later expression of *runx2* strictly corresponds to future cranial bones, with one exception. Transient *runx2* staining appears on the ventromedial corner of the external nares during stage 8 but is absent in later stages (Fig. 4). While this

transient expression might correspond to the future septomaxillary bone, which forms later on the ventrolateral corner of the olfactory organ during stage 13 (Hanken et al. 1992), absence of this staining by stage 10 suggests that it does not. A similar region of cells that surrounds the external nares in *X. laevis* tadpoles also expresses osteogenic markers but does not correlate anatomically to any dermal bone anlagen (R. Kerney, personal observation). Investigation into the function of these putatively osteogenic cells is currently underway.

Limitations of whole mount in situ hybridizations in detecting skeletal anlagen

Early detection of *col2a1* and *sox9* transcripts provides detailed information about the initiation of chondrocyte patterning. However resolution of the morphology of certain cartilage anlagen obtained from these markers is less precise than that obtained from type-II collagen antibody and Alcian blue staining. For instance, cartilages of the lateral braincase (pilae antotica and metotica) were not detectable in any of our in situ hybridizations even though these elements are visible through type-II antibody staining by stage 8 (Hanken et al. 1992). These delicate cartilages form deep within cranial mesenchyme, medial to the eyes. Similarly, hyobranchial skeletal staining is variable using our in situ hybridization methodology in *E. coqui*. For instance, some *col2a1* preparations reveal distinct hyobranchial skeletons (Fig. 2F), while in others the staining is not apparent (Fig. 2H). This lack of detectable staining may be due to the overlying mesenchymal tissues preventing proper penetration of mRNA probes, digoxygenin-conjugated antibodies, or alkaline phosphatase chromagens used in our in situ hybridization protocol. None of the staining patterns described in this study occurs deep within mesenchymal tissues, and all were consistent between replicate samples.

Conclusion

This study uses gene expression to describe early skeletal patterning during cranial development in *E. coqui*. The distribution of *bmp4*, *sox9* and *runx2* links previous studies of neural-crest migration (Moury and Hanken 1995) and gene (Fang and Elinson 1996) and protein (Olsson et al. 2002) expression to later observations of cranial skeletal patterning in a direct-developing anuran (Hanken et al. 1992). Expression of these key skeletal regulators reveals marked repatterning of cranial cartilages as well as transient suprarostral precursors in the frontonasal processes, which never form as distinct cartilages in *E. coqui*. Additionally, expression of *runx2* reveals the early location of osteogenic precursors several stages before they form bone. By examining differentiation markers of chondrogenic and osteogenic cells we find an early instance of developmental repatterning and an unexpected developmental recapitulation in *E. coqui*. These results will inform future studies on the evolutionary changes to genes that mediate cranial patterning (such as the signaling molecule bmp4) or on modifications to thyroid hormone signaling, which may account for the dramatic changes in ontogeny associated with anuran direct development.

Acknowledgments

We thank Brian Hall and Hendrik Müller for reading earlier versions of this manuscript, and the staff of the El Verde field station in Puerto Rico for providing access to their facilities. Anne Everly was extremely helpful in the breeding and maintenance of the frog colony. This material is based upon work supported by the National Science Foundation under grant no. EF-0334846 (AmphibiaTree) to J. H. Ryan Kerney is an American Association of Anatomists Scholar and this research was funded in part by the American Association of Anatomists.

REFERENCES

Abzhanov, A., Protas, M., Grant, B. R., Grant, P. R., and Tabin, C. J. 2004. Bmp4 and morphological variation of beaks in Darwin's finches. *Science* 305: 1462–1465.

Albertson, R. C., Streelman, J. T., Kocher, T. D., and Yelick, P. C. 2005. Integration and evolution of the cichlid mandible: the molecular basis of alternate feeding strategies. *Proc. Natl. Acad. Sci. USA* 102: 16287–16292.

Bell, D. M., et al. 1997. SOX9 directly regulates the type-II collagen gene. *Nat. Genet.* 16: 174–178.

Callery, E. M., and Elinson, R. 2000a. Opercular development and ontogenetic re-organization in a direct-developing frog. *Dev. Genes Evol.* 210: 377–381.

Callery, E. M., and Elinson, R. 2000b. Thyroid hormone-dependent metamorphosis in a direct developing frog. *Proc. Nat. Acad. Sci. USA* 97: 2615–2620.

Depew, M. J., Lufkin, T., and Rubenstein, J. L. 2002. Specification of jaw subdivisions by Dlx genes. *Science* 298: 381–385.

Fang, H., and Elinson, R. P. 1996. Patterns of *distal-less* gene expression and inductive interactions in the head of the direct developing frog *Eleutherodactylus coqui*. *Dev. Biol.* 179: 160–172.

Feduccia, A., and Nowicki, J. 2002. The hand of birds revealed by early ostrich embryos. *Naturwissenschaften* 89: 391–393.

Fell, H. 1925. The histogenesis of cartilage and bone. *J. Morphol. Physiol.* 40: 417–459.

Flores, M. V., Lam, E. Y., Crosier, P., and Crosier, K. 2006. A hierarchy of Runx transcription factors modulate the onset of chondrogenesis in craniofacial endochondral bones in zebrafish. *Dev. Dyn.* 235: 3166–76.

Foppiano, S., Hu, D., and Marcucio, R. S. 2007. Signaling by bone morphogenetic proteins directs formation of an ectodermal signaling center that regulates craniofacial development. *Dev. Biol.* 312: 103–114.

Franssen, R. A., Marks, S., Wake, D. W., and Shubin, N. 2005. Limb chondrogenesis of the seepage salamander, *Desmognathus aeneus* (Amphibia: Plethodontidae). *J. Morphol.* 265: 87–101.

Haas, A. 1996. Non-feeding and feeding tadpoles in hemiphractine frogs: larval head morphology, heterochrony, and systematics of *Flectonotus goeldii* (Amphibia: Anura: Hylidae). *J. Zool. Syst. Evol. Res.* 34: 163–171.

Hall, B. K. 1986. The role of movement and tissue interactions in the development and growth of bone and secondary cartilage in the clavicle of the embryonic chick. *J. Embryol. Exp. Morphol.* 93: 133–152.

Hall, B. K. 2005. *Bones and Cartilage: Developmental and Evolutionary Skeletal Biology*. Elsevier Academic Press, New York.

Hall, B. K., and Miyake, T. 2000. All for one and one for all: condensations and the initiation of skeletal development. *BioEssays* 22: 138–147.

Hanken, J. 1992. Life history and morphological evolution. *J. Evol. Biol.* 5: 549–557.

Hanken, J., and Hall, B. K. 1988. Skull development during anuran metamorphosis: I. Early development of the first three bones to form–the exoccipital, parasphenoid, and frontoparietal. *J. Morphol*. 195: 247–256.

Hanken, J., Klymkowsky, M. W., Alley, K., and Jennings, D. 1997. Jaw muscle development as evidence for embryonic repatterning in direct-developing frogs. *Proc. R. Soc. Lond. B* 264: 1349–1354.

Hanken, J., Klymkowsky, M. W., Summers, C. H., Seufert, D. W., and Ingebrigtsen, N. 1992. Cranial ontogeny in the direct-developing frog, *Eleutherodactylus coqui* (Anura: Leptodactylidae), analyzed using whole mount immunohistochemistry. *J. Morphol*. 211: 95–118.

Heinicke, M., Duellman, W., Trueb, L., Means, D., MacCulloch, R., and Hedges, S. B. 2009. A new frog family (Anura: Terrarana) from South America and an expanded direct-developing clade revealed by molecular phylogeny. *Zootaxa* 2211: 1–35.

Hinchliffe, J., and Griffiths, P. 1982. The prechondrogenic patterns in tetrapod limb development and their phylogenetic significance. In B. Goodwin, N. Holder, and C. Wylie (eds.). *Development and Evolution*. Cambridge University Press, Cambridge, UK, pp. 99–121.

Holmgren, N. 1933. On the origin of the tetrapod limb. *Acta Zool*. 14: 184–295.

Jennings, D., and Hanken, J. 1998. Mechanistic basis of life history evolution in anuran amphibians: thyroid gland development in the direct-developing frog, *Eleutherodactylus coqui*. *Gen. Comp. Endocr*. 111: 225–232.

Kerney, R., Gross, J. B., and Hanken, J. 2007. Runx2 is essential for larval hyobranchial cartilage formation in *Xenopus laevis*. *Dev. Dyn*. 236: 1650–1662.

Kerney, R., Hall, B. K., and Hanken, J. 2010. Regulatory elements of *Xenopus col2a1* drive cartilaginous gene expression in transgenic frogs. *Int. J. Dev. Biol*. 54: 141–150.

Kerney, R., and Hanken, J. 2008. Gene expression reveals unique skeletal patterning in the limb of the direct-developing frog, *Eleutherodactylus coqui*. *Evol. Dev*. 10: 439–448.

Kerney, R., Meegaskumbura, M., Manamendra-Arachchi, K., and Hanken, J. 2007. Cranial ontogeny in *Philautus silus* (Anura: Ranidae: Rhacophorinae) reveals few similarities with other direct-developing anurans. *J. Morphol*. 268: 715–725.

Kimmel, C., DeLaurier, B. A., Ullmann, B., Dowd, J., and McFadden, M. 2010. Modes of developmental outgrowth and shaping of a craniofacial bone in zebrafish. *PLoS One* 5: e9475.

Lev, R., and Spicer, S. 1964. Specific staining of sulphate groups with Alcian blue at low pH. *J. Histochem. Cytochem*. 12: 309.

Linsenmayer, T. F., and Hendrix, M. J. 1980. Monoclonal antibodies to connective tissue macromolecules: type II collagen. *Biochem. Biophys. Res. Commun*. 92: 440–446.

Lynn, W. G. 1942. The embryology of *Eleutherodactylus nubicola*, an anuran which has no tadpole stage. *Contrib. Embryol., Carn. Inst*. 190: 29–90.

Lynn, W. G., and Lutz, B. 1946. The development of *Eleutherodactylus guentheri* STDNR. *Bol. Mus. Nac*. 71: 1–46.

Moriishi, T., Shibata, Y., Tsukazaki, T., and Yamaguchi, A. 2005. Expression profile of *Xenopus* banded hedgehog, a homolog of mouse Indian hedgehog, is related to the late development of endochondral ossification in *Xenopus laevis*. *Biochem. Biophys. Res. Commun*. 328: 867–873.

Moury, D., and Hanken, J. 1995. Early cranial neural crest migration in the direct-developing frog, *Eleutherodactylus coqui*. *Acta Anat*. 153: 243–253.

Nieuwkoop, P. D., and Faber, J. 1994. *Normal Table of Xenopus laevis (Daudin)*. Garland Publishing, New York.

Olsson, L., Moury, D., Carl, T., Håstad, O., and Hanken, J. 2002. Cranial neural crest migration in the direct-developing frog, *Eleutherodactylus coqui*: molecular heterogeneity within and among migratory streams. *Zoology* 105: 3–13.

Orton, G. 1951. Direct development in frogs. *Turtox News* 29: 2–6.

Parsons, K. J., and Albertson, R. C. 2009. Roles for BMP4 and CAM1 in shaping the jaw: evo–devo and beyond. *Annu. Rev. Genet*. 43: 369–388.

Pusey, H. K. 1938. Structural changes to the anuran mandibular arch during metamorphosis, with reference to *Rana temporaria*. *Quart. J. Microsc. Sci*. 80: 479–552.

Reiss, J. O. 1998. Anuran postnasal wall homology: an experimental extirpation study. *J. Morphol*. 238: 343–353.

Roček, Z. 2003. Larval development and evolutionary origin of the anuran skull. In H. Heatwole and M. Davies (eds.). *Amphibian Biology, Vol. 5: Osteology*. Surrey Beatty and Sons, Chipping Norton, Australia, pp. 1877–1995.

Roth, G., and Wake, D. B. 1985. Trends in the functional morphology and sensorimotor control of feeding behavior in salamanders: an example of the role of internal dynamics in evolution. *Acta Biotheor*. 34: 175–192.

Sasano, Y., Zhu J.-X., Kamakura, S., Kusunoki, S., Mizoguchi, I., and Kagayama, M. 2000. Expression of major bone extracellular matrix proteins during embryonic osteogenesis in rat mandibles. *Anat. Embryol*. 202: 31–37.

Sadaghiani, B., and Thiébaud, C. H. 1987. Neural crest development in the *Xenopus laevis* embryo, studied by interspecific transplantation and scanning electron microscopy. *Dev. Biol*. 124: 91–110.

Sampson, L. V. 1900. Unusual modes of breeding and development among anura. *Am. Nat*. 24: 687–715.

Schlosser, G., and Roth, G. 1997. Evolution of nerve development in frogs. II. Modified development of the peripheral nervous system in the direct-developing frog *Eleutherodactylus coqui* (Leptodactylidae). *Brain Behav. Evol*. 50: 94–128.

Searls, R. 1965. An autoradiographic study of the uptake of S35-sulfate during the differentiation of limb bud cartilage. *Dev. Biol*. 11: 155–168.

Semba, I., et al. 2000. Positionally-dependent chondrogenesis induced by BMP4 is co-regulated by Sox9 and Msx2. *Dev. Dyn*. 217: 401–414.

Seufert, D. W., Hanken, J., and Klymkowsky, M. W. 1994. Type II collagen distribution during cranial development in *Xenopus laevis*. *Anat. Embryol*. 189: 81–89.

Shigetani, Y., Nobusada, Y., and Kuratani, S. 2000. Ectodermally derived FGF8 defines the maxillomandibular region in the early chick embryo: epithelial–mesenchymal interactions in the specification of the craniofacial ectomesenchyme. *Dev. Biol*. 228: 73–85.

Shubin, N. H., and Alberch, P. 1986. A morphogenetic approach to the origin and basic organization of the tetrapod limb. In M. K. Hecht, B. Wallace, and G. Prance (eds.). *Evolutionary Biology*. Plenum Press, New York, pp. 319–387.

Spemann, H. 1898. Über die Entwicklung der Tuba Eustachii und des Kopfskelletes von *Rana temporaria*. *Zool. Jahrb*. 11: 389–416.

Spokony, R. F., Aoki, Y., Saint-Germain, N., Magner-Fink, E., and Saint-Jeannet, J. P. 2002. The transcription factor Sox9 is required for cranial neural crest development in *Xenopus*. *Development* 129: 421–432.

Stör, P. 1882. Zur Entwicklung der Anurenschädels. *Z. Wiss. Zool*. 36: 68–103.

Su, M. W., Suzuki, H. R., Bieker, J. J., Solursh, M., and Ramirez, F. 1991. Expression of two nonallelic type II procollagen genes during *Xenopus laevis* embryogenesis is characterized by stage-specific production of alternatively spliced transcripts. *J. Cell Biol*. 115: 565–575.

Swanepoel, J. H. 1970. The ontogenesis of the chondrocranium and of the nasal sac of the microhylid frog *Breviceps adspersus pentheri* (Werner). *Ann. Univ. Stellenbosch (Ser. A)* 45: 1–119.

Trueb, L., and Hanken, J. 1992. Skeletal development in *Xenopus laevis* (Anura: Pipidae). *J. Morphol*. 214: 1–41.

Wada, N., Javidan, Y., Nelson, S., Carney, T. J., Kelsh, R. N., and Schilling, T. F. 2005. Hedgehog signaling is required for cranial neural crest morphogenesis and chondrogenesis at the midline in the zebrafish skull. *Development* 132: 3977–3988.

Wake, D. B., and Roth, G. 1989. The linkage between ontogeny and phylogeny in the evolution of complex systems. In D. B. Wake and G. Roth (eds.). *Complex Organismal Functions: Integration and Evolution in Vertebrates*. John Wiley and Sons Ltd., Chichester, UK, pp. 361–377.

Wake, D., and Shubin, N. 1998. Limb development in the Pacific giant salamanders, *Dicamptodon* (Amphibia, Caudata, Dicamptodontidae). *Can. J. Zool*. 76: 2058–2066.

Welten, M., Verbeek, F., Meijer, A., and Richardson, M. K. 2005. Gene expression and digit homology in the chicken embryo wing. *Evol. Dev*. 7: 18–28.

Wright, E., et al. 1995. The sry-related gene *Sox9* is expressed during chondrogenesis in mouse embryos. *Nat. Genet*. 9: 15–20.

Zelditch, M. 2003. Space, time and repatterning. In B. K. Hall and W. Olson (eds.). *Keywords and Concepts in Evolutionary Developmental Biology*. Harvard University Press, Cambridge, MA, pp. 341–349.